

QUANTIFYING DUNE INTERACTIONS ON PLANETARY SURFACES: UPDATED METHODOLOGY AND IMPLICATIONS FOR DUNE PATTERN ANALYSES. M. C. Marvin¹, A. Gunn^{1,2}, M. Day³, and M. G. A. Lapôtre¹, ¹Department of Geological Sciences, Stanford University, Stanford, CA, USA (mcmarvin@stanford.edu). ²School of Earth, Atmosphere & Environment, Monash University, Clayton, VIC, Australia. ³Department of Earth, Planetary, and Space Sciences, UCLA, Los Angeles, CA, USA.

Introduction: Windblown sand dunes are found on many planetary surfaces in the Solar System, including Venus, Earth, Mars, Titan, Pluto, and the 67P/Churyumov-Gerasimenko comet [1-3], constituting one of the most common landforms in the Solar System. Dune morphology evolves in concert with sediment availability and formative winds (e.g., barchan dunes form under relatively low sediment availability and unidirectional winds). Dunes are composed of a large sand volume relative to the volume of sand mobilized in a given transport event. Therefore, dune morphology reflects the integrated effect of a history of formative winds and sediment supply over relatively long (often > 1 kyr) timescales. Smaller superimposed bedforms, in turn, can provide indications of more recent winds or higher frequency (e.g., seasonal) events. Thus, bedform analyses provide an opportunity to better decipher planetary environments and their history [4].

As dunes collide with one another through time, dune patterns emerge through complex, self-organizing interactions [5-6]. It was previously shown that dunes with longer wavelengths, λ (m), display lower densities of dune defects (defined as the pair of terminations of a given dune) and interactions (defined as points where two dunes have collided or are within 10% of the mean wavelength of each other) [4,7]. As a result, dune interaction density offers a particularly promising avenue to evaluate the age or maturity of planetary dune fields.

Several analyses of dune-field patterns have been conducted before. To date, the most commonly used metrics to quantify the abundance of dune interactions are the defect density, ρ (defined as the number of defect pairs per unit crest length, in m^{-1}) [4] and the interaction density, I (number of interactions per unit area, in m^{-2}) [7]. Both quantities were found to roughly scale with λ^{-2} [7]; however, the latter trend naturally arises when the size of the region that interactions are counted in (or counting area) is correlated with wavelength – even if the average number of interactions per dune were to be invariant – highlighting the need for a refined approach to quantifying the density of dune interactions.

A new approach to quantifying dune interactions: We define the average number of interactions per dune within a dune field,

$$\alpha = \frac{n}{N} \quad (1)$$

where n is the number of interactions and N the total number of dunes within the counting area. To decouple the extent of counting areas with dune wavelength, we first identified the largest portion within a dune field where dune wavelength was roughly homogenous and traced a circle of area half of that of the dune field that contains that portion. Correlating the surface area of the counting area with dune field extent instead of dune wavelength ensures that our analysis does not reflect a simple geometric artifact of methodologies. Using a circle instead of a square or rectangle also allows to eliminate any bias related to the dunes' migration direction relative to the shape of the counting area.

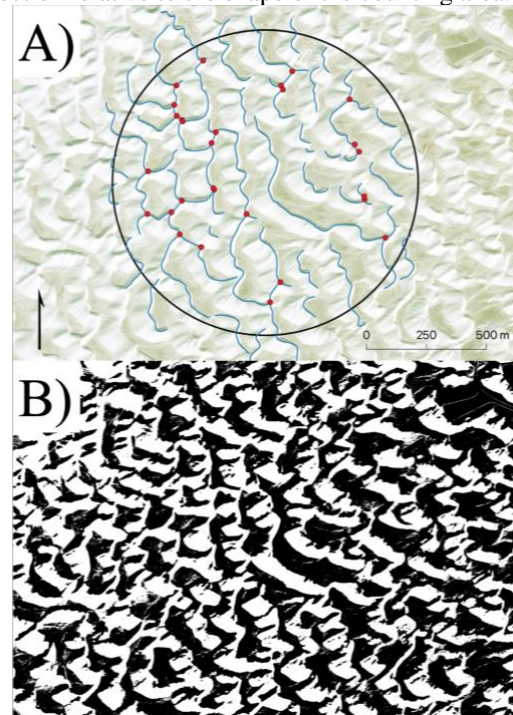


Figure 1: (A) Dune crestlines (blue lines), counting area (black circle), and interactions (red dots) at White Sands National Park. (B) Binary thresholding of dune field imagery, with white denoting sand cover and black interdune areas.

Because the extent of counting areas is not correlated with dune wavelength, some dunes are not fully contained within the counting circle; we thus report N as a decimal value, where partial dunes are reported as the fraction of their crestline length contained within the circle (Fig. 1A). We define a dune interaction as points where dune terminations are within < 10% of the

average λ from each other [7] (evaluated from >35 crestline-normal measurements of λ per dune field and through the creation of a buffer polygon around the full length of every single dune crestline).

Using the described methodology, we compiled λ , α , I , and dune density (# dunes per surface area) for a total of 20 terrestrial dune fields, including ten fields of crescentic dunes and ten of linear dunes. In addition, we calculated the fractional surface area of sand cover within the counting area through binary thresholding of each counting area image (Fig. 1B); a fractional sand-cover of 1 implies that the bed is fully covered in windblown sand, whereas values < 1 imply that interdune areas are not covered with loose sand.

Preliminary results: We find that the number of interactions per dune, α , does not significantly vary with dune wavelength, λ . In other words, the number of interactions per dune is not expected to necessarily evolve as dunes become more widely spaced through time, regardless of dune type (Fig. 2). As the density of dunes increases, α increases as well – a trend that makes intuitive sense as dune terminations are expected to get closer to each other when more dunes are contained within a given counting area (Fig. 3). Fractional sand cover also shows promise as a potential control on α , with α following the same decreasing trend with fractional sand cover irrespective of dune type (Fig. 4).

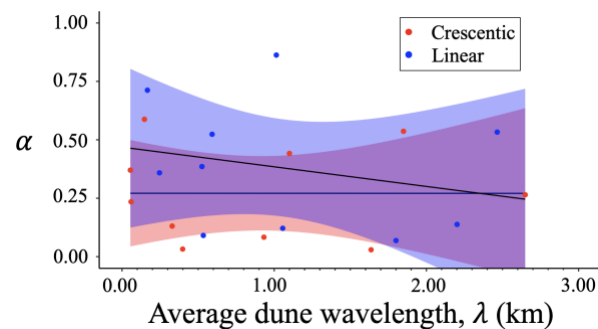


Figure 2: Average number of interactions per dune as a function of average dune wavelength. Shaded areas highlight the 95% confidence of best-fit power-law regressions (black lines).

Future Work and Conclusion: The same analysis will be conducted for a variety of crescentic and linear dune fields on Mars from the global Context Camera (CTX) mosaic of [8]. We will first focus on dune fields in the Olympia Undae and Nili Patera regions.

Building on and improving upon previous studies of dune interactions, our preliminary analysis of terrestrial dune fields provides a jumping-off point to better understand the mechanistic controls on the abundance

of dune interactions, and ultimately, to decipher the history of planetary surfaces from orbiter-based imagery.

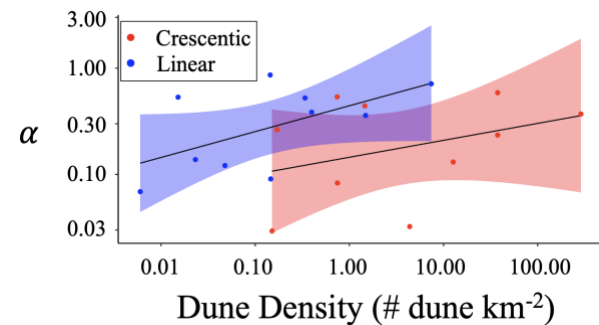


Figure 3: Average number of interactions per dune as a function of dune density within the dune field. Shaded areas highlight the 95% confidence intervals of best-fit power-law regressions (black lines).

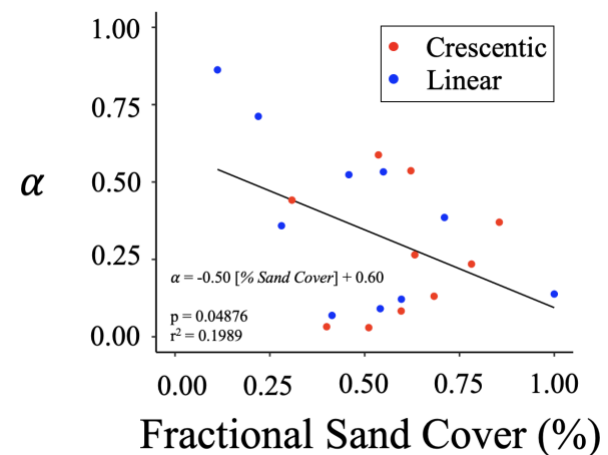


Figure 4: Average number of interactions per dune as a function of fractional sand cover. Best-fit regression includes both linear and crescentic dunes.

References: [1] Bourke M.C. et al., (2010) *Geomorphology*, 121(1-2), 1-14. [2] Telfer M.W. et al., (2018) *Science*, 360(6392), 992–997. [3] Thomas N. et al., (2015) *Astro. Astrophys.*, 583, A17. [4] Ewing R.C. et al., (2015) *Nature Geoscience*, 8(1), 15-19. [5] Werner B.T. (1997) *Geology*, 23, 1107–1110. [6] Werner B.T. and Kocurek G. (1999) *Geology*, 27, 727–730. [7] Day M. and Kocurek G. (2018) *Geology*, 46, 999–1002. [8] Dickson J. L. et al., (2018) *LPSC*, 49.